

DMD #40030

The Impact of Intestinal Glucuronidation on the Pharmacokinetics of Raloxifene

Keigo Kosaka, Norifumi Sakai, Yuya Endo, Yuga Fukuhara, Minoru Tsuda-Tsukimoto,
Tatsuyuki Ohtsuka, Ichiro Kino, Tomohiko Tanimoto, Naomi Takeba, Masakatsu Takahashi,
and Toshiyuki Kume

DMPK Research Laboratory, Mitsubishi Tanabe Pharma Corporation, Saitama, Japan: K.K.,
Y.F., M.TT., T.O., I.K., T.T., N.T., M.T., T.K.

Drug Metabolism and Analysis Department, Mitsubishi Chemical Medience Corporation,
Ibaraki, Japan: N.S., Y.E.

DMD #40030

Running title: Intestinal and Hepatic Availabilities of UGT Substrates

Corresponding Author: Keigo Kosaka

Mailing address: DMPK Research Laboratory, Mitsubishi Tanabe Corporation, 2-2-50,
Kawagishi, Toda-shi, Saitama, 335-8505, Japan

Phone: +81-48-433-8101

Fax: +81-48-433-8170

E-mail: Kosaka.Keigo@ma.mt-pharma.co.jp

Number of Text pages = 44

No. of Tables = 4

No. of Figures = 5

No. of references = 38

No. of words in Abstract = 248

No. of words in Introduction = 668

No. of words in Discussion = 1493

Abbreviations used are: AUC, Area under the curve; CYP, Cytochrome P450; CL_h, Hepatic
blood clearance; CL_{int}, Intrinsic clearance; Eisai hyperbilirubinemic rats; F, Oral

DMD #40030

bioavailability; Fa, Fraction of absorption; Fg, Intestinal availability; Fh, Hepatic availability; fu, Fraction unbound; G6P, Glucose 6-phosphate; G6P-DH, Glucose-6-phosphate dehydrogenase; IVIVC, In vitro-in vivo correlation; LC-MS/MS, Liquid chromatography/tandem mass spectrometry; Mic., Microsomes; MRP, Multidrug resistance-associated protein; NCE, new chemical entity; PBS, phosphate buffer solution; P-gp, P-glycoprotein; P.V., Portal vein; Qh, Hepatic blood flow; Qpv, blood flow in the portal vein; Rb, Blood to plasma concentration ratio; SD, Sprague-Dawley; Sys., Systemic; UGT, UDP-glucuronosyltransferase

DMD #40030

Abstract

Raloxifene is extensively glucuronidated in humans, effectively reducing its oral bioavailability (2%). It was also reported to be glucuronidated in pre-clinical animals, but its effects on the oral bioavailability have not been fully elucidated. In the present study, raloxifene and its glucuronides in the portal and systemic blood were monitored in Gunn rats deficient in uridine diphosphate-glucuronosyltransferase (UGT) 1A, Eisai hyperbilirubinemic rats (EHBRs), which hereditarily lack multidrug resistance-associated protein (MRP) 2, and wild-type rats after oral administration. The in vitro–in vivo correlation (IVIVC) of four UGT substrates (raloxifene, biochanin A, gemfibrozil, and mycophenolic acid) in rats was also evaluated. In Gunn rats, the product of fraction absorbed and intestinal availability, and hepatic availability of raloxifene were 0.63 and 0.43, respectively; these values were twice of those observed in wild-type Wistar rats, indicating that raloxifene was glucuronidated in both the liver and intestine. The ratio of glucuronides to unchanged drug in systemic blood was substantially higher in EHBRs (129-fold) than in the wild-type Sprague–Dawley rats (10-fold), suggesting the excretion of raloxifene glucuronides caused by MRP2. The IVIVC of the other UGT substrates in rats displayed a good relationship, but the oral clearance values of raloxifene and biochanin A, which were extensively glucuronidated by rat intestinal microsomes, were higher than the predicted clearances using rat liver microsomes, suggesting that intestinal metabolism may be a great contributor to the first-pass effect. Therefore, evaluation of

DMD #40030

intestinal and hepatic glucuronidation for new chemical entities is important to improve their pharmacokinetic profiles.

DMD #40030

Introduction

Glucuronidation is a phase II metabolic reaction catalyzed by uridine diphosphate (UDP)–glucuronosyltransferase (UGT) that transforms endogenous substances and xenobiotics into more hydrophilic compounds that are subsequently eliminated through excretion of urine and/or bile. Most lipophilic drugs are initially metabolized by cytochrome P450 (CYP). Therefore, during the discovery stage of new chemical entities (NCEs), pharmaceutical companies focus more on preventing the metabolism of these drugs by P450. However, over the last decade, more hydrophilic compounds have been synthesized and new concerns regarding UGT-catalyzed metabolism have been revealed because these processes are important for detoxification and prolongation of efficacy of some drugs. UGTs are widely expressed in various tissues including the liver, kidney, and gastrointestinal tract, implying that extrahepatic metabolism may exert a critical influence on the pharmacokinetics of glucuronidated drugs. It is well known that phenolic compounds including opioid analgesics such as morphine and flavonoids are extensively glucuronidated in the liver and small intestine (Ritter et al., 2007). In some cases, poor oral bioavailability (F) of the drugs is attributed to the susceptibilities to glucuronidation. Therefore, extrapolation of in vitro glucuronidation data to in vivo pharmacokinetic parameters is essential but difficult due to the complex nature of UGT enzymes (Lin et al., 2002). Several studies on in vitro–in vivo correlation (IVIVC) for UGT substrates have been published recently (Kilford et al., 2009;

DMD #40030

Miners et al., 2010). It was reported that in vitro predictability depends on enzyme sources, experimental conditions, and the occurrence of atypical glucuronidation kinetics, and thus selection of an appropriate approach is a key point to predict pharmacokinetics successfully.

F of raloxifene, a selective estrogen receptor modulator used in the treatment of osteoporosis, in humans has been reported as only 2% (Eli Lilly Clinical data; Mizuma, 2009).

UGT1A8 and 1A10, isozymes that are absent in the human liver, are thought to glucuronidate raloxifene mainly in the intestine and lead to extremely low F (Jeong et al., 2005; Kemp et al., 2002). F of raloxifene in rats and dogs were originally reported as 39% and 17%, respectively (Lindstrom et al., 1984), and have been recently reported as 4% and 0%, respectively (Deguchi et al., 2011). The UGT isozymes responsible for the glucuronidation of raloxifene and its intestinal and hepatic availabilities (F_g and F_h, respectively) in preclinical animals have not been investigated adequately. It has been reported that raloxifene and its conjugates were excreted into the bile and gut lumen by P-glycoprotein (P-gp) and/or multidrug resistance-associated proteins (MRPs), and these efflux transports are considered to participate in the long-lasting enteric recycling of this drug (Jeong et al., 2004; Xu et al., 2009). Currently, human UGT isoforms responsible for glucuronidating some drugs are being investigated in detail, however, much less is known about UGTs in animals, species differences in the intestinal and hepatic glucuronidation, and subsequent excretion of glucuronides.

DMD #40030

In the present study, raloxifene and its glucuronides were monitored in the portal and systemic blood after oral administration in rats and dogs, and the product of fraction absorbed and intestinal availability ($F_a \cdot F_g$) and F_h were estimated. This approach confirmed the species differences in $F_a \cdot F_g$ and F_h of raloxifene. The in vitro intestinal and hepatic intrinsic clearance values, which were corrected to $CL_{int, u}$ using microsomal binding in the incubation mixture, were determined using rat, dog, monkey, and human microsomes fortified with UDPGA or NADPH, and the IVIVCs were also examined. To clarify the involvement of UGT1As in the glucuronidation of raloxifene and the role of MRP2 in the excretion of its glucuronides, the pharmacokinetic profiles of raloxifene in UGT1A-deficient rats (Gunn rats) and Eisai hyperbilirubinemic rats (EHBRs), which hereditarily lack MRP2, were compared with those of their wild-type (Wistar and Sprague–Dawley (SD)) rats. Furthermore, the IVIVCs of several other compounds (biochanin A, mycophenolic acid, and gemfibrozil), which are mainly eliminated through glucuronidation in rats, were also investigated. The purpose of this study was to examine the usefulness of in vitro microsomal assays of intestinal and hepatic glucuronidation in improving the pharmacokinetic profiles of NCEs during drug discovery.

DMD #40030

Materials and Methods

Reagents

Raloxifene, β -glucuronidase (Type IX-A, from *Escherichia coli*), glucose 6-phosphate (G6P), and β -nicotinamide adenine dinucleotide phosphate (NADP) were purchased from Sigma-Aldrich (MO, USA). Mycophenolic acid, biochanin A, gemfibrozil, and ethylenediaminetetraacetic acid (EDTA) were purchased from Wako Pure Chemical (Osaka, Japan). Glucose-6-phosphate dehydrogenase (G6P-DH) and protease inhibitor cocktail tablets (Complete, EDTA-free) were purchased from Roche (Mannheim, Germany). The UGT reaction mix solution (250 mM Tris-HCl, 40 mM MgCl₂, 0.125 mg/ml alamethicin) was purchased from BD Gentest (NJ, USA). Liver and intestinal microsomes from SD rats, beagle dogs, cynomolgus monkeys, and humans were obtained from XenoTech (KS, USA). All chemicals were analytical grade or the highest quality available.

Animals

All animal procedures were conducted under protocols approved by the Mitsubishi Tanabe Institutional Animal Care and Use Committee. Eight-week old male Wistar, SD, Gunn rats, and EHBRs were obtained from Japan SLC (Shizuoka, Japan). Male SD rats (9–10-week old) with catheters implanted in the portal and jugular vein were obtained from Charles River Japan (Yokohama, Japan). Rats were kept in a temperature- and humidity-controlled

DMD #40030

environment and were allowed to acclimate for 1 week before use. Male beagle dogs (7–17-month old) were obtained from Kitayama Labs (Nagano, Japan). Male cynomolgus monkeys (42–61-month old) were obtained from Nafovanny (Dong Nai, Vietnam). These animals were housed in Mitsubishi Chemical Medience facilities where the temperature and humidity were controlled.

Preparation of microsomes

To compare the metabolic activities of different strains of rats, liver, and intestinal microsomes from SD, EHBRs, Wistar and Gunn rats were prepared (pooled, $n = 3$). Rat liver microsomes were prepared using standard techniques (von Moltke et al., 1993). In brief, pooled microsomes from three individuals were prepared by ultracentrifugation (11,900g for 20 min and 104,700g for 1 h twice). Microsomal pellets were resuspended in 0.1 M phosphate buffer solution (PBS) (pH 7.4) containing 20% glycerol. Total protein concentration was determined using a bicinchoninic acid (BCA) protein assay kit (Thermo Fisher Scientific, USA) using bovine serum albumin (BSA) as a standard. The prepared microsomes were stored at 80°C until use. Rat intestinal microsomes were prepared as described in a previous study by another group (Perloff et al., 2004). In brief, after exsanguination, 15-cm sections of the upper intestines from the duodenum to the jejunum were immediately isolated, and the intestinal segments were flushed and incubated in solution A (pH 7.3) containing 1.5 mM KCl, 96 mM

DMD #40030

NaCl, 27 mM sodium citrate, 9.6 mM PBS, and protease inhibitor (20 tablets/l) with bubbling oxygen for 15 min at 4°C. The intestinal segments were filled with solution B (pH 7.0) containing 1.5 mM KCl, 96 mM NaCl, 1.5 mM EDTA, 1 mM dithiothreitol, 0.1% BSA, 9.6 mM PBS, and protease inhibitor (20 tablets/l). After tapping the intestinal segments on an ice-cooled plate for 2 min to peel the epithelial cells off the intestinal wall, the suspension in the lumen were collected. The suspension was centrifuged at 800g for 10 min and the resulting pellets were resuspended in solution C (pH 7.0) containing 5 mM histidine, 0.25 M sucrose, 0.5 mM EDTA, and protease inhibitor (20 tablets/l). The cell pellets were washed with solution C and homogenized and centrifuged at 15,000g for 10 min. The supernatant was collected and 5 volumes of 52 mM CaCl₂ were added. The tubes containing microsomes were gently mixed, allowed to stand for 15 min, and centrifuged at 2,000g for 10 min. The resulting microsomal pellets were suspended in solution D (pH 7.4) containing 20% glycerol, 10 mM EDTA, and 0.1M Tris-HCl buffer. The total protein concentration was determined by the BCA protein assay, and the microsomes were stored at -80°C until use.

Microsomal incubation

CL_{int} was determined using the substrate depletion method ($n = 3-5$). Substrate solutions were prepared at a final concentration of 2 μM in dimethylsulfoxide and acetonitrile (0.01% and 0.99% final concentrations, respectively) except for gemfibrozil (10 μM final

DMD #40030

concentration). The substrates were incubated in 96-well plates and placed on a heating block at 37°C. The suspensions containing microsomes (0.5 mg/ml of protein except for biochanin A; 0.1 mg/ml of protein) were either dispensed into the 50 mM-Tris-HCl solution (pH 7.5) with 25 µg/ml alamethicin and 8 mM MgCl₂ for UGT reactions, or into the 72.5-mM PBS with 5 mM MgCl₂ and 1 mM EDTA for CYP reactions as final concentrations. The suspensions were vortexed, allowed to stand for 10 min in the heating block, and the metabolism assay was initiated by addition of 2 mM UDPGA or the NADPH-generating system containing 1 mM NADP, 10 mM G6P, and 2 units/ml of G6P-DH as final concentrations. All assays were incubated for a maximum of 60 min, and reactions were terminated with 4 volumes of acetonitrile containing 0.1% formic acid and verapamil as the internal standard (IS). The samples were then centrifuged and the supernatant was filtered and transferred to the other 96-well plates for analysis using a liquid chromatography/tandem mass spectrometry (LC-MS/MS) as system described below.

Microsomal binding

The unbound fraction in rat liver microsomal suspensions (f_u , mic) was determined in triplicate by ultracentrifugation. The microsomes were suspended in 72.5 mM PBS at the same concentration as that used for metabolic stability experiments. The samples for binding studies were centrifuged at 436,000g for 4 h at 37°C, and aliquots of the centrifuged upper

DMD #40030

fraction were transferred into 15 volumes of acetonitrile containing IS. Standard samples containing the same matrices were prepared, and the unbound compound concentrations in the incubation mixtures were quantified using LC-MS/MS.

Plasma protein binding

The unbound fraction in rat plasma (f_u, p) was determined in triplicate by equilibrium dialysis using a serum binding system (BD Gentest, NJ, USA). Plasma samples were spiked with the test compound (10- μ M final concentration), and the device containing plasma and PBS was reciprocated in a CO₂ incubator at 37°C for 20 h. The resulting PBS samples were transferred into 8 volumes of acetonitrile containing IS. Standard samples containing the same matrices were prepared, and the unbound compound concentration in the plasma was quantified using LC-MS/MS.

Blood to plasma concentration ratio

Blood to plasma concentration ratio (R_b) was determined in vitro after incubation of the compounds with fresh rat blood in duplicate. Blood was warmed to 37°C, and the test compound was spiked at a 10- μ M final concentration. The blood samples were incubated at 37°C for 5 min and divided into two portions. After centrifugation of the aliquot, the plasma and blood samples were transferred into 4 volumes of acetonitrile containing IS, centrifuged,

DMD #40030

and filtered. Standard samples containing the same matrices were prepared, and the compound concentration in plasma and blood was quantified by LC-MS/MS.

Pharmacokinetic studies in animals

Raloxifene (1 mg/kg body weight) was dissolved in a solution containing ethanol, polyethyleneglycol 300, and water (1:4:5) as reported previously (Lindstrom et al., 1984) and intravenously administered (i.v.) at a volume of 0.5 ml/kg to fasted SD, Wistar, EHBRs, and Gunn rats ($n = 3$). Blood samples were collected from the animals at 0.05, 0.25, 0.5, 1, 2, 4, 8, and 24 h after dosing. The plasma samples were separated by centrifugation and stored at -20°C . The plasma samples were processed for analysis by protein precipitation with acetonitrile containing IS, followed by centrifugation and filtration. Standard samples containing the same matrices were prepared, and the compound concentrations in the plasma were quantified using LC-MS/MS. For monitoring raloxifene concentrations in portal and systemic plasma after oral administration (p.o.), SD rats cannulated in the portal and jugular vein were used. Raloxifene (2 mg/kg body weight) was dissolved in the same solution as used for intravenous administration at a volume of 4 ml/kg ($n = 3-4$), and blood samples were collected at 0.25, 0.5, 1, 2, 4, 8, and 24 h after dosing. For monitoring drug concentrations in portal and systemic plasma after oral administration to EHBRs, Wistar, and Gunn rats, all animals were sacrificed at 5 or 6 time points ($n = 3$), and blood samples were

DMD #40030

corrected. Intravenous ($n = 2$) or oral ($n = 3$) administration of raloxifene to beagle dogs was conducted using the same solution as that administered to the rats, and pharmacokinetic profile studies in cynomolgus monkeys were performed in the same manner ($n = 2$). When raloxifene was studied in dogs, pharmacokinetic parameters before and after cannulation in the portal vein were compared. The other UGT substrates, biochanin A (50 mg/kg, p.o.), mycophenolic acid (10 mg/kg, p.o.), and gemfibrozil (30 mg/kg, p.o.) were administered to intact SD rats (i.v.) or cannulated SD rats (p.o.) under the same conditions used for raloxifene ($n = 3$). The preparation of plasma samples was as described above except for gemfibrozil, for which the collected plasma samples were immediately transferred to acetonitrile (containing 0.1% formic acid) and IS to avoid degradation of its acyl glucuronide.

Quantification of glucuronides

The glucuronide concentrations of raloxifene and biochanin A were estimated through a hydrolysis assay using β -glucuronidase. The samples were incubated in the presence of 250 units of β -glucuronidase at 37°C for 12–15 h, and the completion of hydrolysis was ascertained by LC-MS/MS analysis. The glucuronide concentration of gemfibrozil was determined by UV detection without a hydrolysis assay, where it was assumed that the UV absorbances of the unchanged drug and glucuronide were the same. Because only traces of mycophenolic acid glucuronides were detected by UV, these were not quantified.

DMD #40030

LC-MS/MS analysis

Qualitative analysis for the identification of metabolites was performed using an HP1100 system (Agilent Technologies, CA) equipped with a triple quadrupole Quattro Micro mass spectrometer (Waters, MA). LC conditions were as follows: column temperature, 40°C; column, CAPCELL PACK MGII (2.0 mm I.D. × 150 mm, 3 μm, Shiseido, Japan); gradient elution at 0.2 ml/min, with acetonitrile and 10 mM ammonium acetate; UV detection, 290 nm; run time, 20 min. The main working parameters for mass spectrometers were as follows: ion mode, ESI, positive and negative; capillary voltage, 3 kV; cone voltages, 20 and 40 V; source temperature, 100°C; desolvation temperature, 350°C. The quantitative analysis for unchanged compounds was performed using an Acquity UPLC system equipped with a triple quadrupole mass spectrometer, Xevo TQ MS (Waters, MA). UPLC conditions were set as follows: column temperature, 50°C; column, Waters Acquity UPLC BEH C18 (2.1 mm I.D. × 30 mm, 1.7 μm); gradient elution at 0.5 ml/min, with acetonitrile and 10 mM ammonium acetate; run time, 3 min. The parameters for mass spectrometers were as follows: ion mode, ESI, positive for raloxifene, biochanin A, and mycophenolic acid, negative for gemfibrozil; multi-reaction monitoring method with transitions of m/z 474 → 112 for raloxifene, m/z 285 → 213 for biochanin A, m/z 321 → 159 for mycophenolic acid, and m/z 249 → 121 for gemfibrozil; capillary voltage, 0.5 kV; cone voltage and collision energy, 50 V and 30 eV for

DMD #40030

raloxifene, 50 V and 40 eV for biochanin A, 40 V and 35 eV for mycophenolic acid, 20 V and 30 eV for gemfibrozil; source temperature, 150°C; and desolvation temperature, 600°C.

Estimation of F_h, F_a*F_g, and F

F_h was calculated by dividing the systemic plasma AUCs (AUC_{sys}) by the portal plasma AUCs (AUC_{pv}) after oral administration to animals. F_a*F_g was estimated using Equation 1:

$$F_a * F_g = Q_{pv} * R_b * (AUC_{pv} - AUC_{sys}) / \text{Dose} \quad (1)$$

where Q_{pv} is the blood flow in the portal vein, which was assumed to be 70% of the hepatic blood flow (Q_h) set at 55 ml/min/kg body weight for rats or 31 ml/min/kg body weight for dogs (Davies et al., 1993). F was calculated by multiplying F_h and F_a*F_g when AUC_{pv} was available. If AUC_{pv} was not available, F was calculated by dividing the oral AUC by the intravenous AUC normalized with dose.

IVIVC of UGT substrates in rats

Data from incubations with either CYP or UGT cofactors were analyzed using a nonlinear single exponential fit, and the CL_{int} values (ml/min/mg protein) were calculated from the elimination rate constant k, volume of incubation, and amount of microsomal protein in

DMD #40030

incubation. Obtained CL_{int} values were corrected for experimentally determined f_u, mic to give $CL_{int, u}$ and were scaled to the whole body clearance, $CL_{int, h}$ (ml/min/kg body weight) for rats using Equation 2:

$$CL_{int, h} = k * 50 \text{ mg microsomes/g liver} * 37.8 \text{ g liver/kg body weight} \quad (2)$$

microsomes concentration * f_u, mic

where 50 mg microsomes/g liver was a scaling factor (Iwatsubo et al., 1996; Zhou et al., 2002) and 37.8 g liver/kg body weight was the liver weight used (Luttringer et al., 2003).

The observed hepatic clearance values after intravenous administration were converted to $CL_{int, iv}$ values using the well-stirred or parallel tube liver models, defined in Equations 3 and 4, respectively:

$$\text{Observed } CL_{int, iv} = CL_b / f_u, p * R_b / (1 - CL_b / Q_h) \quad (3)$$

$$\text{Observed } CL_{int, iv} = - Q_h / f_u, p * R_b * \ln (1 - CL_b / Q_h) \quad (4)$$

where CL_b is the hepatic blood clearance. For biochanin A, the calculated CL_b value exceeded the Q_h , and therefore, CL_b was assumed as 90% of the hepatic blood flow as

DMD #40030

reported previously by another group (Cubitt et al., 2009). The renal clearance of the four compounds used in this study was minor; therefore, hepatic clearance was assumed to be equal to the total clearance. The observed $CL_{int, po}$ was calculated from the oral plasma clearance using Equation 5, which assumed complete absorption and no intestinal metabolism:

$$\text{Observed } CL_{int, po} = CL_{po}/f_{u, p} * R_b \quad (5)$$

DMD #40030

Results

In vitro hepatic and intestinal intrinsic clearance of raloxifene

The in vitro $CL_{int, u}$ values of raloxifene were estimated using liver and intestinal microsomes (XenoTech) fortified with NADPH or UDPGA. The final values were corrected with the free fraction in microsomal incubation ($f_{u, mic}$, 0.278) (Table 1). The in vitro $CL_{int, u}$ values for glucuronidation determined with intestinal microsomes were higher than those with liver microsomes among the tested species, and the values using human intestinal microsomes were the highest. In contrast, the in vitro $CL_{int, u}$ values for CYP-catalyzed metabolism were higher with liver microsomes than with intestinal microsomes for these species.

The liver and intestinal microsomes were prepared from SD, Wistar, EHBRs, and Gunn rats and the in vitro $CL_{int, u}$ values of raloxifene were compared. As expected, the in vitro $CL_{int, u}$ for glucuronidation determined with Gunn rat microsomes was significantly lower than that with Wistar rat microsomes (Fig. 1A). The in vitro $CL_{int, u}$ values for CYP metabolism in EHBRs and Gunn rats were lower than those in SD and Wistar rats, respectively (Fig. 1B).

Pharmacokinetics of raloxifene

LC-MS/MS analysis with UV detection (290 nm) of the SD rat portal plasma samples at 15 min after oral administration of raloxifene resulted in the appearance of two glucuronide

DMD #40030

peaks as major metabolites (Fig. 2). Other metabolites such as sulfated or oxidized raloxifene were less. After incubation of this plasma sample in the presence of β -glucuronidase, the two major peaks disappeared. The plasma concentration versus time curves of raloxifene and its glucuronides in SD rats showed rapid absorption and extensive glucuronidation (Fig. 3A). $F_a \cdot F_g$ and F_h in SD rats were estimated at 0.16 and 0.33, respectively, and the AUC ratio of glucuronides to the unchanged drug was 5.73 and 9.67 in the portal and systemic plasma, respectively (Table 2). The pharmacokinetics in Gunn and wild-type Wistar rats exhibited significant differences (Fig. 3B and 3D). $F_a \cdot F_g$ and F_h in Gunn rats were 0.63 and 0.43, respectively; these values were twice of those observed (0.34 and 0.20, respectively) in Wistar rats. The AUC ratio of glucuronides to unchanged drug in the portal plasma was 2.51 in Wistar rats and 0.03 in Gunn rats. The plasma concentration of raloxifene glucuronides in EHBRs was dramatically higher than wild-type SD rats (Fig. 3A and 3C). The AUC ratio of glucuronides to unchanged drug in EHBRs was 46.8 in the portal plasma and 129 in the systemic plasma (Table 2).

The PK parameters of raloxifene in beagle dogs were examined before and after implanting catheters in the portal vein. The total clearance and F were similar between before and after the cannulation. $F_a \cdot F_g$ and F_h in dogs were estimated at 0.36 and 0.16, respectively (Fig. 3E and Table 2). F in dogs (0.044 and 0.052) was comparable to F in SD rats (0.048), but the AUC ratios of glucuronides to unchanged drug were lower in dogs (portal, 0.27; systemic,

DMD #40030

1.34) than in rats (portal, 5.73; systemic, 9.67). F in cynomolgus monkeys was also comparable (0.030) with those in rats and dogs, but the AUC ratios of glucuronides to unchanged drug in systemic plasma were higher in monkeys (85.0) than in rats and dogs (Fig. 3F and Table 2).

IVIVC of other UGT substrates in rats

The in vitro $CL_{int, u}$ values of biochanin A, mycophenolic acid, and gemfibrozil were determined using rat liver and intestinal microsomes (Table 3). The $CL_{int, u}$ values of biochanin A for glucuronidation were extremely high in both rat liver and intestinal microsomes. The $CL_{int, u}$ values of mycophenolic acid for glucuronidation were higher in rat intestinal microsomes than in rat liver microsomes. In contrast, $CL_{int, u}$ values of gemfibrozil for glucuronidation were lower in rat intestinal microsomes than in rat liver microsomes. In all cases, the in vitro $CL_{int, u}$ values for CYP metabolism were less than those for glucuronidation. The in vitro hepatic $CL_{int, u}$ values for glucuronidation were scaled to whole body clearance values (ml/min/kg body weight) and were compared with the observed in vivo CL_{int} values obtained from both intravenous and oral pharmacokinetic data (Fig. 4). For calculation of the in vivo CL_{int} values, the following R_b , plasma protein binding, and f_u , mic values were incorporated. The R_b values for gemfibrozil, mycophenolic acid, raloxifene, and biochanin A were 0.56, 0.63, 1.07, and 0.75, respectively. The plasma protein binding values for these

DMD #40030

compounds were 98.9, 99.2, 99.4, and 98.8%, respectively. The f_u , f_{mic} values for these compounds were 0.907, 0.776, 0.278, and 0.600, respectively. The IVIVC from intravenous clearance values was relatively good, but the $CL_{int, h}$ values of raloxifene and biochanin A obtained from the oral pharmacokinetic data were significantly underestimated, supporting the contribution of intestinal metabolism to a first-pass effect. $F_a \cdot F_g$ and F_h of biochanin A, mycophenolic acid, and gemfibrozil were examined after oral administration to SD rats (Table 4). Biochanin A, which is susceptible to extremely high glucuronidation, exhibited low $F_a \cdot F_g$ (0.15), whereas gemfibrozil and mycophenolic acid, compounds with relatively low CL_{int} for glucuronidation, demonstrated high $F_a \cdot F_g$ (1.40 and 1.17, respectively).

DMD #40030

Discussion

Conjugation reactions have been increasingly recognized as important metabolic processes that play a strong role in the pharmacokinetics of some drugs; therefore, prediction of the clearance of such drugs is necessary. However, unlike CYP substrates, the IVIVC for UGT substrates has not been studied adequately because the amount of UGTs expressed in tissues is uncertain and the intraluminal localization of the catalytic sites, which require activation for *in vitro* glucuronidation, makes IVIVC more complex (Lin et al., 2002). UGTs are widely expressed in various tissues including the liver, kidney, and gastrointestinal tract (Ohno et al., 2009), and the importance of extrahepatic glucuronidation has been reported (Ritter et al., 2007). Flavonoids (polyphenolic phytochemicals) were employed as model UGT substrates in several studies where not only hepatic but also intestinal glucuronidation and subsequent excretion by efflux transporters were reported (Jia et al., 2004; Zhang et al., 2007).

Raloxifene also has phenolic groups, and its oral bioavailability in humans is very low because of a high glucuronidation rate catalyzed by UGT1A8 and 1A10 in the intestine (Kemp et al., 2002; Jeong et al., 2005; Mizuma, 2009); its conjugates are subsequently excreted into the gut lumen by P-gp and/or MRPs. These enzyme and transporter couplings are thought to result in long half lives due to enteric recycling despite the extensively high oral clearance (Jeong et al., 2004; Xu et al., 2009).

DMD #40030

In the present study, species differences in $CL_{int, u}$ for in vitro glucuronidation of raloxifene were investigated (Table 1), and the results were compared with its pharmacokinetics (Table 2). To activate UGT, alamethicin was employed as a pore-forming agent according to previous reports (Dalvie et al., 2008; Cubitt et al., 2009). The results were consistent with those reported by others where the glucuronidation rates with rat or human intestinal microsomes were higher than those with rat or human liver microsomes. Our study also showed that all the $CL_{int, u}$ values among investigated animals were higher for glucuronidation than for P450 metabolism in intestinal microsomes. The $CL_{int, u}$ values obtained with dog liver or intestinal microsomes were comparable to those with rat liver or intestinal microsomes. Comparing these in vitro $CL_{int, u}$ values with the $Fa \cdot Fg$ and Fh values in the two animals demonstrated a reasonable relationship. In humans and monkeys, the raloxifene concentrations in portal plasma were not available; therefore, $Fa \cdot Fg$ was calculated from intravenous and oral pharmacokinetic data (total clearance in human = 0.647 l/hr/kg, Eli Lilly Clinical data) by assuming $Fh = 1 - CL_b/Qh$ and $Fa \cdot Fg = F/Fh$. When Qh values in humans and monkeys were set at 20.7 and 43.6 ml/min/kg (Davies et al., 1993), the calculated $Fa \cdot Fg$ values were 0.045 and 0.041, respectively. The Fa of raloxifene in humans was reported as 0.63 (Eli Lilly Clinical data) and its permeability was high in our in-house study using Caco-2 cells (data not shown). Therefore, intestinal glucuronidation must be a main factor contributing to the first-pass effect.

DMD #40030

In the present study using Gunn and Wistar rats, glucuronidation of raloxifene by UGT1As was suggested (Fig. 3B and 3D, and Table 2). The $F_a \cdot F_g$ and F_h values in Gunn rats were 2-fold higher than those in Wistar rats, respectively, indicating that raloxifene was glucuronidated in the intestine as well as in the liver. In the comparison of EHBRs with SD rats (Fig. 3A and 3C), the differences in $F_a \cdot F_g$ and F_h were small, and the ratio of glucuronides to unchanged drug in systemic plasma was much higher in EHBRs, suggesting that the excretion of raloxifene glucuronides was influenced by MRP2. Some groups have reported a compensatory up-regulation of enzymes and transporters in Gunn and MRP2-deficient TR rats (Kim et al., 2003; Wang et al., 2009). Flavonoids such as apigenin are efficiently metabolized by Gunn rats because of compensatory up-regulation of intestinal UGT 2Bs and hepatic efflux transporters, which increases their disposition and limits their oral bioavailabilities. In our studies, $CL_{int, u}$ values for CYP metabolism determined with liver microsomes from Gunn rats and EHBRs were lower than those from Wistar and SD rats (Fig. 2); therefore, CYPs responsible for the oxidation of raloxifene did not show compensatory up-regulation. $CL_{int, u}$ values for glucuronidation determined with microsomes from Gunn rats were lower than those from Wistar rats; implying that UGTs responsible for glucuronidation of raloxifene were not up-regulated. Interestingly, species differences in the ratio of glucuronides to unchanged drugs were observed despite comparable $CL_{int, u}$ values for glucuronidation in dogs, rats, and monkeys. These ratios in the systemic plasma in dogs, SD rats, and monkeys

DMD #40030

were 1.34–1.84, 9.67, and 85.0, respectively, and the ratio in humans was reported as 70–90 (Eli Lilly Clinical data). The ratios in monkeys and humans were closer to those in EHBRs than those in wild-type SD rats, indicating that excretion of raloxifene glucuronides into the intestinal lumen and bile may significantly differ among these species. Expression of MRP2 in rat, dog, and human intestine has been reported (Mottino et al., 2000; Conrad et al., 2001), but species differences in transport activity of raloxifene glucuronides have not been reported. A schematic representation of the intestinal and hepatic disposition of raloxifene is presented in Fig. 5. Further studies are needed to understand the differences in raloxifene glucuronide levels in circulation after administration in these species.

The *in vitro* hepatic $CL_{int, u}$ values of raloxifene, biochanin A, mycophenolic acid, and gemfibrozil (Table 3) for glucuronidation were scaled to whole body clearances (ml/min/kg body weight) and compared with their observed *in vivo* CL_{int} (Fig. 4 and Table 4). These compounds have been reported to be mainly excreted in bile as glucuronides in rats (Curtis et al., 1985; Jia et al., 2004; Takekuma et al., 2007). Therefore, their total clearance values were assumed to be nearly equal to their hepatic clearance values. The $CL_{int, h}$ values could be predicted quite well from the *in vitro* hepatic $CL_{int, u}$ values for glucuronidation except raloxifene. $CL_{int, u}$ value of raloxifene with rat liver microsomes in the presence of NADPH was comparable to that in the presence of UDPGA; this underestimation may be caused by the exploration which was not incorporated CYP-catalyzed metabolism into hepatic clearance.

DMD #40030

The oral clearance values for raloxifene and biochanin A were much higher than the predicted values, implying that intestinal glucuronidation was a great contributor. The *in vitro* intestinal $CL_{int, u}$ values for glucuronidation relatively corresponded to the $F_a \cdot F_g$ values for the four compounds investigated. Biochanin A is also a human UGT 1A10 substrate, which is considered to be an important isoform in the gastrointestinal tract (Lewinsky et al., 2005). With regard to this compound, much less is known about the intestinal effect on pre-systemic elimination in humans and the responsible UGT isoforms in rats. There are several publications on IVIVC for UGT substrates (Kilford et al., 2009; Miners et al., 2010). It is well known that *in vitro* predictability of CL_{int} depends on enzyme sources, experimental conditions, and the occurrence of atypical glucuronidation kinetics. In some cases, *in vitro* CL_{int} values using microsomes were underestimated in comparison with *in vivo* values. It was reported that addition of BSA to the incubation improved the predictability from microsomal data in particular for UGT2B7 substrates (Rowland et al., 2007; 2008). However, Kilford et al. reported that human CL_{int} value of gemfibrozil, UGT 2B7 substrate, was overestimated 10-fold when BSA was added to the microsomal incubation. In the present study, rat CL_{int} value of gemfibrozil was successfully predicted using rat liver microsomes in the absence of BSA. Rat UGT isoforms responsible for glucuronidating gemfibrozil and their selectivity of substrates have not been fully elucidated, therefore further studies are needed. Recently, models for F_g prediction of drugs, particularly for CYP 3A substrates, which are metabolized

DMD #40030

in the small intestine, have been proposed (Galetin et al., 2006; Yang et al., 2007; Gertz et al., 2010; Kadono et al., 2010). These approaches have not been applied extensively to UGT substrates, which are eliminated through species- and/or tissue-dependent glucuronidation. In most pharmaceutical companies, NCEs not susceptible to CYP-catalyzed metabolism have been eagerly investigated and synthesized by introducing hydrophilic groups into their structures. Therefore, prediction of F_g for such compounds, which are often eliminated through phase II metabolism and subsequent excretion, is becoming essential. For anionic compounds, the interactions of conjugating enzymes with transporters have been increasingly recognized as an important process of elimination (Nies et al., 2008; Pang et al., 2009; Sun et al., 2010). Therefore, comprehensive studies including metabolism and transport are required.

In conclusion, the impact of Intestinal glucuronidation on the pharmacokinetics of UGT substrates was investigated by in vitro and in vivo methods. The contribution of intestinal and hepatic glucuronidation of raloxifene to first-pass effect was demonstrated in rats and dogs. The Pharmacokinetic studies in EHBRs indicated the excretion of raloxifene glucuronides by MRP2 which is possibly different among animals. The in vitro intestinal CL_{int} corresponded with $F_a \cdot F_g$ for UGT substrates examined in rats. Therefore, evaluation of intestinal and hepatic glucuronidation for NCEs is important to improve their pharmacokinetic profiles.

DMD #40030

Acknowledgments

We thank Charles River Japan for offering cannulated SD rats.

DMD #40030

Authorship Contributions

Participated in research design: Kosaka, Sakai, Endo, Fukuhara, Tsuda-Tsukimoto, and Kume.

Conducted experiments: Kosaka, Sakai, Endo, Fukuhara, Tsuda-Tsukimoto, Ohtsuka, Kino, Tanimoto, Takeba, and Takahashi.

Contributed new reagents or analytic tools: Kosaka, and Fukuhara.

Performed data analysis: Kosaka.

Wrote or contributed to the writing of the manuscript: Kosaka, and Kume.

DMD #40030

References:

Conrad S, Viertelhaus A, Orzechowski A, Hoogstraate J, Gjellan K, Schrenk D, and Kauffmann HM (2001) Sequencing and tissue distribution of canine MRP2 gene compared with MRP1 and MDR1. *Toxicology* **156**: 81–91.

Cubitt HE, Houston JB, and Galetin A (2009) Relative Importance of Intestinal and Hepatic Glucuronidation—Impact on the Prediction of Drug Clearance. *Pharm Res* **26**: 1073–1083.

Curtis CG, Danaher TM, Hibbert EA, Morris CL, Scott AM, Woolcott BA, and Powell GM (1985) The fate of gemfibrozil and its metabolites in the rat. *Biochem Soc Trans*, **13**: 1190–1191.

Dalvie D, Kang P, Zientek M, Xiang C, Zhou S, and Obach RS (2008) Effect of intestinal glucuronidation in limiting hepatic exposure and bioactivation of raloxifene in humans and rats. *Chem Res Toxicol*, **21**: 2260–2271.

Davies B and Morris T (1993) Physiological parameters in laboratory animals and humans. *Pharm Res*, **10**: 1093–1095.

DMD #40030

Deguchi T, Watanabe N, Kurihara A, Igeta K, Ikenaga H, Fusegawa K, Suzuki N, Murata S, Hirouchi M, Furuta Y, Iwasaki M, Okazaki O, and Izumi T (2011) Human pharmacokinetics prediction of UDP-glucuronosyltransferase substrates with an animal scale-up approach.

Drug Metab Dispos **39**: 820-829.

Galetin A and Houston JB (2006) Intestinal and hepatic metabolic activity of five cytochrome P450 enzymes: impact on prediction of first-pass metabolism. *J Pharmacol Exp Ther* **318**: 1220–1229.

Gertz M, Harrison A, Houston JB, and Galetin A (2010) Prediction of human intestinal first-pass metabolism of 25 CYP3A substrates from In Vitro clearance and permeability data.

Drug Metab Dispos **38**: 1147–1158.

Iwatsubo T, Hirota N, Ooie T, Suzuki H, and Sugiyama Y (1996) Prediction of In Vivo drug disposition from In Vitro data based on physiological pharmacokinetics. *Biopharm Drug Dispos* **17**: 273–310.

Jeong EJ, Lin H, and, Hu M (2004) Disposition mechanisms of Raloxifene in the human intestinal Caco-2 model. *J Pharmacol Exp Ther* **310**: 376–385.

DMD #40030

Jeong EJ, Liu Y, Lin H, and Hu M (2005) Species- and disposition model-dependent metabolism of raloxifene in gut and liver: role of UGT1A10. *Drug Metab Dispos* **33**: 785–794.

Jia X, Chen J, Lin H, and Hu M (2004) Disposition of Flavonoids via enteric recycling: Enzyme-Transporter coupling affects metabolism of Biochanin A and Formononetin and excretion of their phase II conjugates. *J Pharmacol Exp Ther* **310**: 1103-1113.

Kadono K, Akabane T, Tabata K, Gato K, Terashita S, and Teramura T (2010) Quantitative prediction of intestinal metabolism in Humans from a simplified intestinal availability model and empirical scaling factor. *Drug Metab Dispos* **38**: 1230-1237.

Kemp DC, Fan PW, and Stevens JC (2002) Characterization of Raloxifene glucuronidation in vitro: Contribution of intestinal metabolism to presystemic clearance. *Drug Metab Dispos* **30**: 694–700.

Kilford PJ, Stringer R, Sohal B, Houston JB, and Galetin A (2009) Prediction of drug clearance by glucuronidation from in vitro Data: Use of combined cytochrome P450 and UDP-Glucuronosyltransferase cofactors in alamethicin-activated human liver microsomes.

DMD #40030

Drug Metab Dispos **37**: 82–89.

Kim MS, Liu DQ, Strauss JR, Capodanno I, Yao Z, Fenyk-Melody JE, Franklin RB, and Vincent SH (2003) Metabolism and disposition of gemfibrozil in Wistar and multidrug resistance-associated protein 2-deficient TR- rats. *Xenobiotica* **33**: 1027–1044.

Lewinsky RH, Smith PA, and Mackenzie PI (2005) Glucuronidation of bioflavonoids by human UGT1A10: structure–function relationships. *Xenobiotica* **35**: 117-129.

Lin JH and Wong BK (2002) Complexities of glucuronidation affecting In vitro-In vivo extrapolation. *Curr Drug Metab* **3**: 623–646.

Lindstrom TD, Whitaker NG, Whitaker GW (1984) Disposition and metabolism of a new benzothiophene antiestrogen in rats, dogs and monkeys. *Xenobiotica* **14**: 841–847.

Luttringer O, Theil FP, Poulin P, Schmitt-Hoffmann AH, Guentert TW, and Lave T (2003) Physiologically based pharmacokinetic (PBPK) modeling of disposition of epiroprim in humans. *J Pharm Sci* **92**: 1990–2007.

DMD #40030

Miners JO, Mackenzie PI, and Knights KM, (2010) The prediction of drug-glucuronidation parameters in humans: UDP-glucuronosyltransferase enzyme selective substrate and inhibitor probes for reaction phenotyping and in vitro–in vivo extrapolation of drug clearance and drug-drug interaction potential. *Drug Metab Rev* **42**: 196–208.

Mizuma T (2009) Intestinal glucuronidation metabolism may have a greater impact on oral bioavailability than hepatic glucuronidation metabolism in humans: A study with raloxifene, substrate for UGT1A1, 1A8, 1A9, and 1A10. *Int J Pharm* **378**: 140–141.

Mottino AD, Hoffman T, Jennes L, and Vore M (2000) Expression and localization of Multidrug Resistant Protein Mrp2 in rat small intestine. *J Pharmacol Exp Ther* **293**: 717-723.

Nies AT, Schwab M, and Keppler D (2008) Interplay of conjugating enzymes with OATP uptake transporters and ABCC/MRP efflux pumps in the elimination of drugs. *Expert Opin Drug Metab Toxicol* **4**: 545–568.

Ohno S and Nakajin S, (2009) Determination of mRNA expression of human UDP-Glucuronosyltransferases and application for localization in various human tissues by real-time reverse transcriptase-polymerase chain reaction. *Drug Metab Dispos* **37**: 32–40.

DMD #40030

Pang KS, Maeng H and Fan (2009) Interplay of transporters and enzymes in drug and metabolite processing. *Mol Pharm*, **6**: 1734-1755.

Perloff MD, Von Moltke LL, and Greenblatt DJ (2004) Ritonavir and dexamethasone induce expression of CYP3A and P-glycoprotein in rats. *Xenobiotica* **34**: 133-150.

Ritter JK, (2007) Intestinal UGTs as potential modifiers of pharmacokinetics and biological responses to drugs and xenobiotics. *Expert Opin Drug Metab Toxicol* **3**: 93–107.

Rowland A, Gaganis P, Elliot DJ, Mackenzie PI, Knights KM, and Miners JO (2007) Binding of inhibitory fatty acids is responsible for the enhancement of UDP-glucuronosyltransferase 2B7 activity by albumin: implications for in vitro-in vivo extrapolation. *J Pharmacol Exp Ther* **321**: 137–147.

Rowland A, Knights KM, Mackenzie PI, and Miners JO (2008) The “albumin effect” and drug glucuronidation: bovine serum albumin and fatty acid-free human serum albumin enhance the glucuronidation of UDP-glucuronosyltransferase (UGT) 1A9 substrates but not UGT1A1 and UGT1A6 activities. *Drug Metab Dispos* **36**: 1056–1062.

DMD #40030

Takekuma Y, Kakiuchi H, Yamazaki K, Miyauchi S, Kikukawa T, Kamo N, Ganapathy V, and Sugawara M (2007) Difference between pharmacokinetics of mycophenolic acid (MPA) in rats and that in humans is caused by different affinities of MRP2 to a glucuronized form. *J Pharm Pharm Sci* **10**: 71–85.

Sun H, Zeng YY, and Pang KS (2010) Interplay of phase II enzymes and transporters in futile cycling: Influence of multidrug resistance-associated protein 2-mediated excretion of estradiol 17B-D-glucuronide and its 3-sulfate metabolite on net sulfation in perfused TR- and Wistar rat liver preparations. *Drug Metab Dispos* **38**:769-780.

Von Moltke, L. L., Greenblatt, D. J., Harmatz, J. S. and Shader, R. I. (1993) Alprazolam metabolism in vitro: studies of human, monkey, mouse, and rat liver microsomes. *Pharmacology* **47**: 268-276.

Wang SWJ, Kulkarni KH, Tang L, Wang JR, Yin T, Daidoji T, Yokota H, and Hu M (2009) Disposition of flavonoids via enteric recycling: UDP-glucuronosyltransferase (UGT) 1As deficiency in Gunn rats is compensated by increases in UGT2Bs activities. *J Pharmacol Exp Ther*, **329**: 1023–1031.

DMD #40030

Xu H, Kulkarni KH, Singh R, Yang Z, Wang SWJ, Vincent H. Tam, and Ming Hu (2009)

Disposition of Naringenin via glucuronidation pathway is affected by compensating efflux transporters of hydrophilic glucuronides. *Mol Pharm* **6**: 1703–1715.

Yang J, Jamei M, Yeo KR, Tucker GT, and Rostami-Hodjegan A (2007) Prediction of intestinal first-pass drug metabolism. *Curr Drug Metab* **8**: 676-684.

Zhang L, Zuo Z, and Lin G (2007) Intestinal and hepatic glucuronidation of Flavonoids. *Mol Pharm* **4**: 833–845.

Zhou SF, Tingle MD, Kestell P and Paxton JW (2002) Species differences in the metabolism of the antitumour agent 5,6-dimethylxanthone-4-acetic acid in vitro: implications for prediction of metabolic interactions in vivo. *Xenobiotica* **32**: 87–107.

DMD #40030

Figure Legends

Fig. 1. The $CL_{int, u}$ of raloxifene metabolism (ml/min/mg protein) in rat microsomes. Microsomal incubations were fortified with UDPGA (A) or NADPH (B). Closed and open columns represent $CL_{int, u}$ by liver and intestinal microsomes, respectively. Each column represents the mean, and error bars are the standard deviations of the mean.

Fig. 2. HPLC chromatograms with UV detection at 290 nm of raloxifene and its metabolites: (A) rat blank plasma; (B) portal plasma at 15 min after dosing raloxifene (2 mg/kg, p.o.) to SD rats.

Fig. 3. Plasma concentration versus time profiles of raloxifene and its glucuronides after oral administration. Closed and open symbols represent the systemic and portal plasma concentrations, respectively. Triangle and square symbols represent raloxifene and its glucuronides, respectively. Raloxifene was dissolved in ethanol, polyethyleneglycol 300, and water (1:4:5) and administered at 2 mg/kg to SD rats (A), Wistar rats (B), EHBRs (C), Gunn rats (D), beagle dogs (E), and cynomolgus monkeys (F). Each symbol represents the mean, and the error bars are the standard deviations of the mean.

Fig. 4. Comparison of predicted and observed $CL_{int, h}$ values in SD rats. $CL_{int, h}$ values were

DMD #40030

predicted using rat liver microsomes fortified with UDPGA: (A) comparisons of predicted and observed $CL_{int, h}$ values from intravenous pharmacokinetic data obtained from the well-stirred (open) and parallel tube (closed) liver models for four compounds; (B) comparison of predicted and observed $CL_{int, h}$ values from oral pharmacokinetic data that assumed complete absorption and no intestinal metabolism. Dashed lines represent $Y = X$.

Fig. 5. Schematic representation of intestinal and hepatic disposition of raloxifene.

S and G represent raloxifene and glucuronic acid, respectively.

DMD #40030

Table 1. $CL_{int, u}$ of raloxifene metabolism (ml/min/mg protein) by rat, dog, monkey, and human liver and intestinal microsomes. Microsomal incubations were fortified with UDPGA or NADPH. $CL_{int, u}$ values represent the mean of three determinations and the standard deviations of the mean.

Microsomes	$CL_{int, u}$ (ml/min/mg, protein)							
	UGT				CYP			
	Liver		Intestine		Liver		Intestine	
Rat	0.359	± 0.038	0.992	± 0.099	0.293	± 0.096	0.019	± 0.007
Dog	0.693	± 0.086	1.344	± 0.088	0.884	± 0.033	0.092	± 0.012
Monkey	0.289	± 0.075	1.737	± 0.692	0.386	± 0.027	0.375	± 0.009
Human	0.470	± 0.051	3.284	± 0.268	0.119	± 0.022	0.028	± 0.008

DMD #40030

Table 2. Pharmacokinetic parameters of raloxifene after intravenous or oral administration to SD rats, EHBRs, Wistar rats, Gunn rats, beagle dogs, and cynomolgus monkeys. In cases where AUC_{pv} was not available (intact dogs and monkeys), F was calculated by dividing the oral AUCs by the intravenous AUCs corrected for dose. Values in parentheses represent standard deviations and ND means not determined.

Animals	1 mg/kg, i.v.				2 mg/kg, p.o.					
	CL _{tot}	V _{dss}	AUC	C _{max}	AUC	Glu / Parent ratio		F _h	Fa*F _g	F
	(ml/h/kg)	(ml/kg)	(ng·h/ml)	(ng/ml)	(ng·h/ml)	portal	systemic			
SD rats	2051 (172)	3240 (440)	490 (42)	11.4 (0.7)	58.3 (15.2)	5.73 (1.14)	9.67 (4.65)	0.33 (0.11)	0.16 (0.08)	0.048 (0.014)
EHBRs	1323 (153)	3673 (499)	762 (84)	14.5	160	46.8	129	0.43	0.26	0.113
Wistar rats	1475 (323)	4015 (1673)	704 (176)	13.0	68.2	2.51	3.80	0.20	0.34	0.067
Gunn rats	1305 (158)	4967 (595)	775 (100)	45.2	389	0.03	0.09	0.43	0.63	0.272
Dogs										
intact	1057	3157	976	16.0 (2.3)	85.7 (15.6)	ND	1.84 (0.61)	ND	ND	0.044 (0.008)
cannulated	1163	3022	860	23.3 (1.4)	87.4 (20.9)	0.27 (0.10)	1.34 (0.52)	0.16 (0.04)	0.36 (0.18)	0.052 (0.014)
Monkeys	909	3847	1102	6.0	62.2	ND	85.0	ND	ND	0.026

DMD #40030

Table 3. $CL_{int, u}$ of gemfibrozil, mycophenolic acid, raloxifene, and biochanin A metabolism (ml/min/mg protein) by rat liver and intestinal microsomes. Microsomal incubations were fortified with UDPGA or NADPH. $CL_{int, u}$ values represent the mean of three determinations and the standard deviations of the mean.

Compounds	$CL_{int, u}$ (ml/min/mg, protein)							
	UGT				CYP			
	Liver		Intestine		Liver		Intestine	
Gemfibrozil	0.273	± 0.008	0.001	± 0.002	0.025	± 0.008	0.002	± 0.002
Mycophenolic acid	0.042	± 0.006	0.229	± 0.014	0.006	± 0.003	0.002	± 0.001
Raloxifene	0.359	± 0.038	0.992	± 0.099	0.293	± 0.096	0.019	± 0.007
BiochaninA	5.050	± 0.744	2.845	± 0.234	0.062	± 0.004	0.004	± 0.004

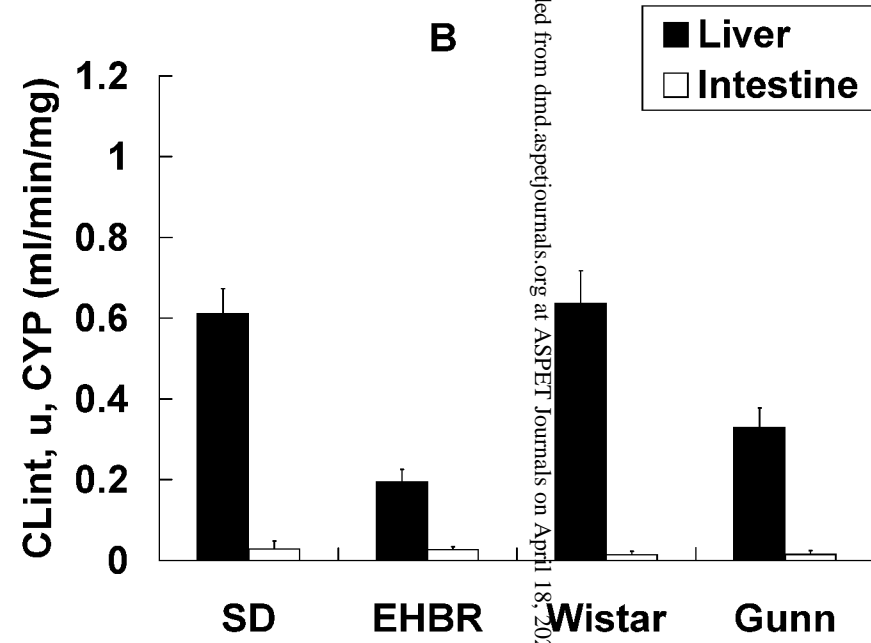
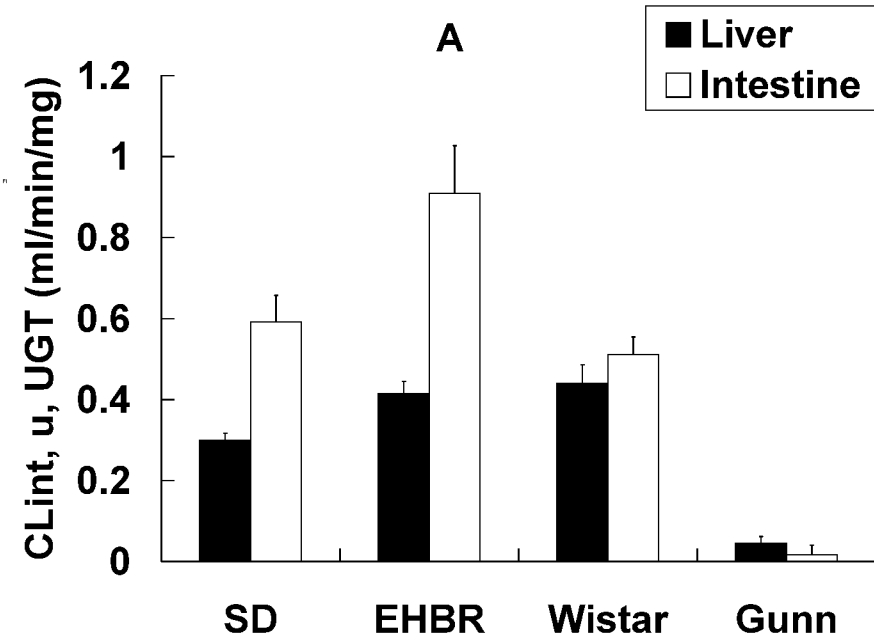
DMD #40030

Table 4. Pharmacokinetic parameters of gemfibrozil, mycophenolic acid, raloxifene, and biochanin A after intravenous or oral administration to SD rats. Values in parentheses represent standard deviations and ND means not determined. In the case of mycophenolic acid, the standard deviation was not calculated because the difference between systemic and portal AUCs was too small; therefore, Fa*Fg was estimated from each averaged AUC.

compounds	intravenous				oral							
	Dose (mg/kg)	CL _{tot} (ml/h/kg)	V _{dss} (ml/kg)	AUC (ng·h/ml)	Dose (mg/kg)	C _{max} (ng/ml)	AUC (ng·h/ml)	Glu / Parent ratio		Fh	Fa*Fg	F
								portal	systemic			
Gemfibrozil	3	437 (154)	2234 (1397)	7626 (3244)	30	44583 (31358)	62320 (20397)	0.17 (0.03)	0.18 (0.01)	0.65 (0.16)	1.40 (0.64)	0.85 (0.19)
Mycophenolic acid	3	107 (49)	637 (265)	34366 (20858)	10	46901 (2900)	135027 (23271)	ND	ND	0.94	1.17	1.10
Raloxifene	1	2051 (172)	3240 (440)	490 (42)	2	11.4 (0.7)	58.3 (15.2)	5.73 (1.14)	9.67 (4.65)	0.33 (0.11)	0.16 (0.08)	0.048 (0.01)
Biochanin A	5	3228 (527)	938 (465)	1578 (265)	50	6.0 (2.2)	69.9 (34.4)	2.98 (0.99)	110 (73)	0.016 (0.008)	0.15 (0.06)	0.0024 (0.0012)

Downloaded from dmd.aspetjournals.org at ASPET Journals on April 18, 2024

Figure 1



Downloaded from dnd.aspejournals.org at ASPET Journals on April 18, 2024

Figure 2

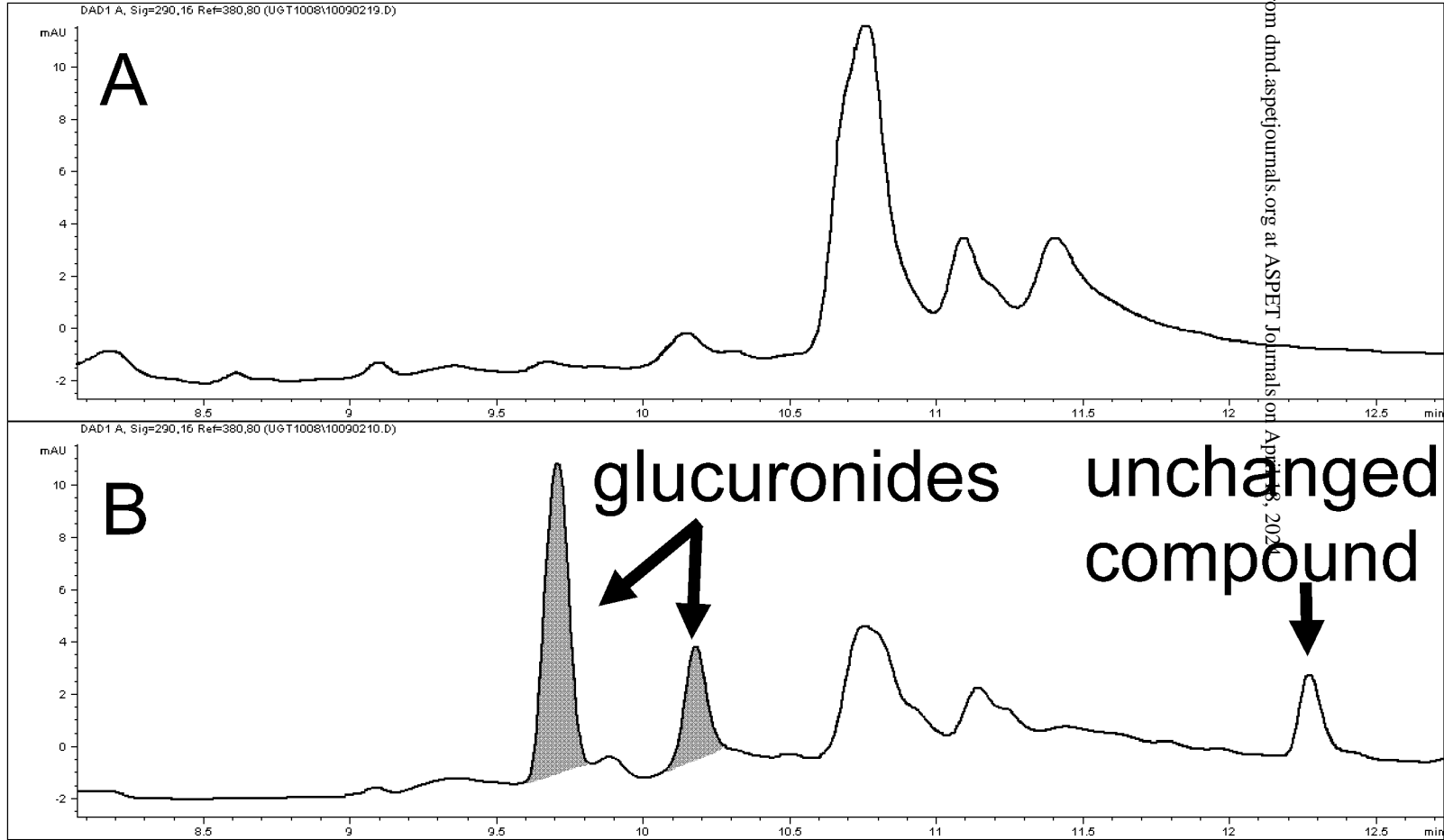


Figure 3

DMD Fast Forward. Published on June 6, 2011 as DOI: 10.1124/dmd.111.040030
This article has not been copyedited and formatted. The final version may differ from this version.

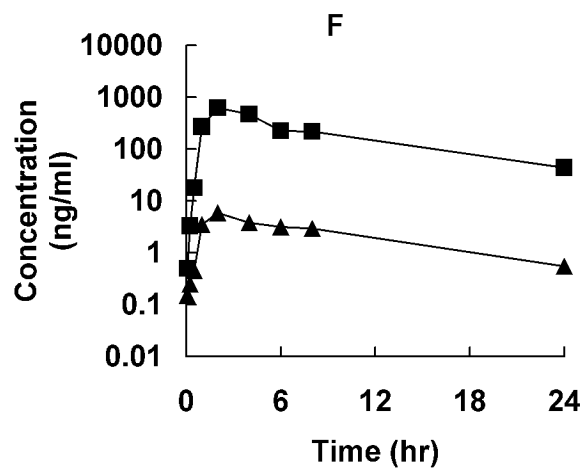
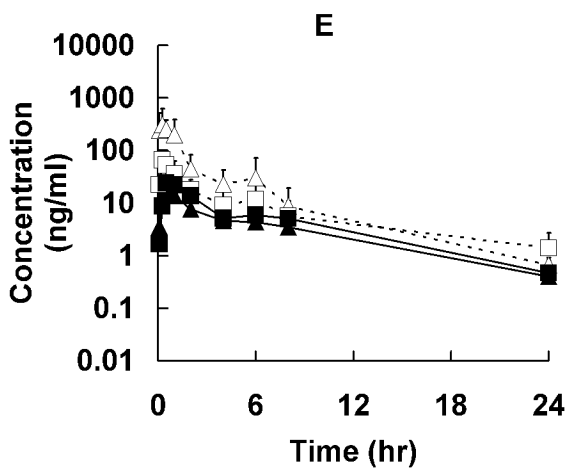
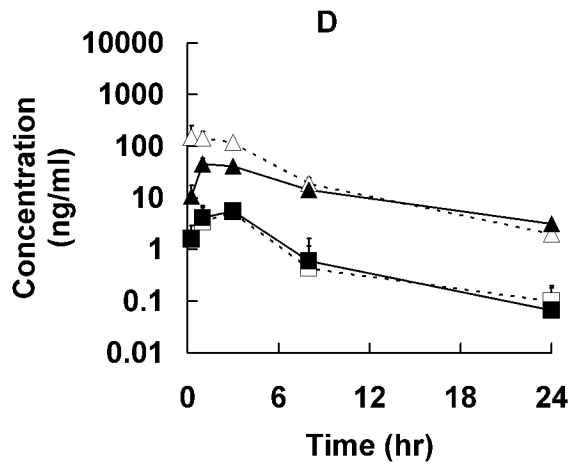
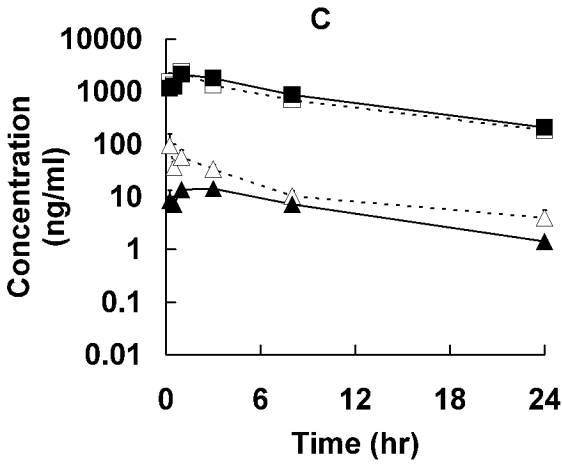
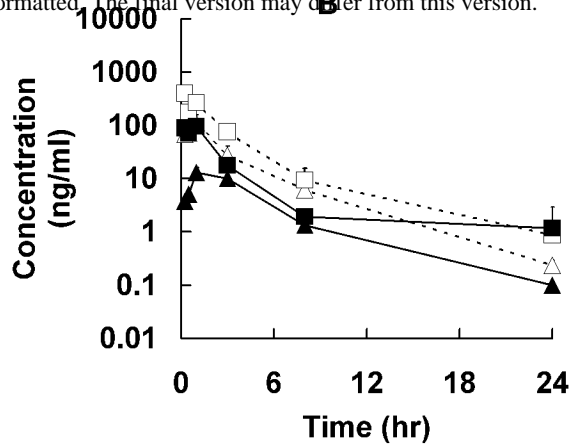
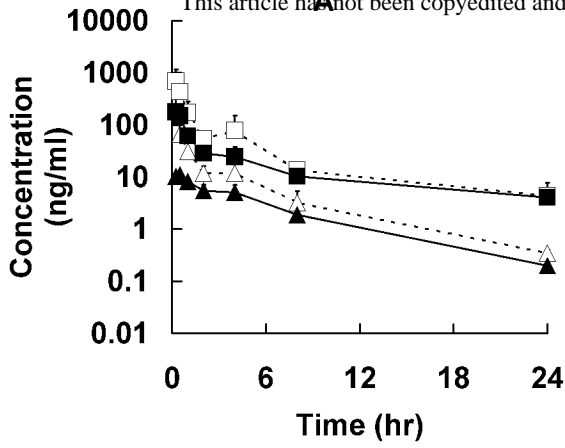
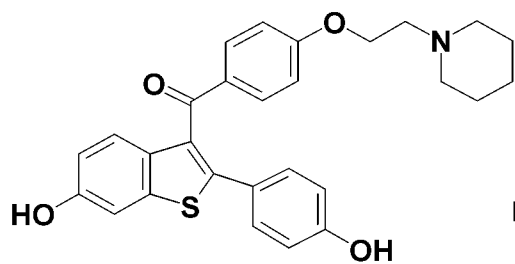
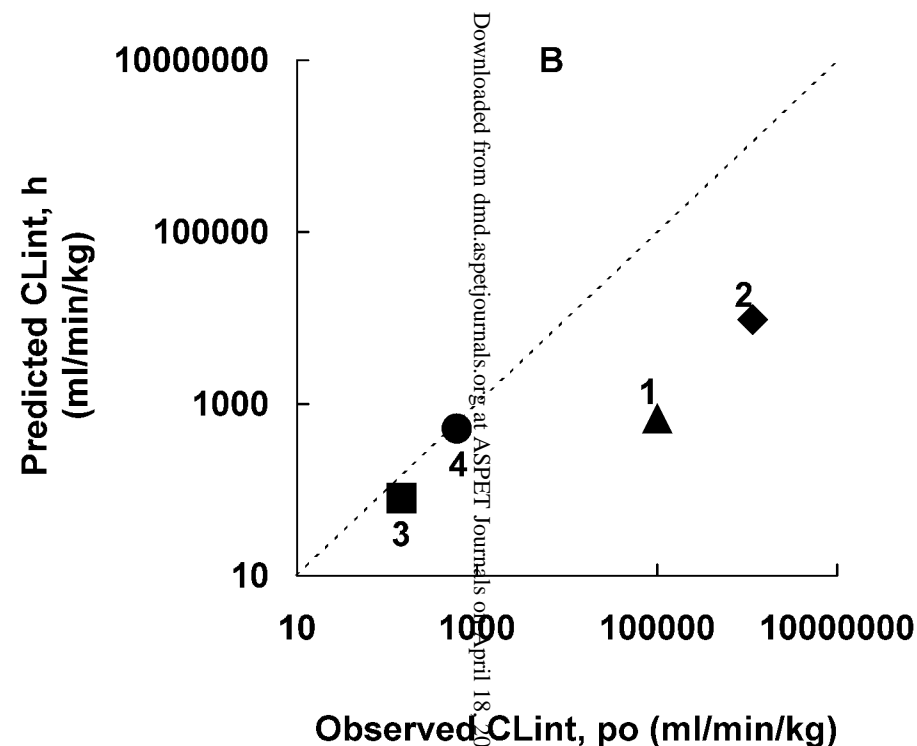
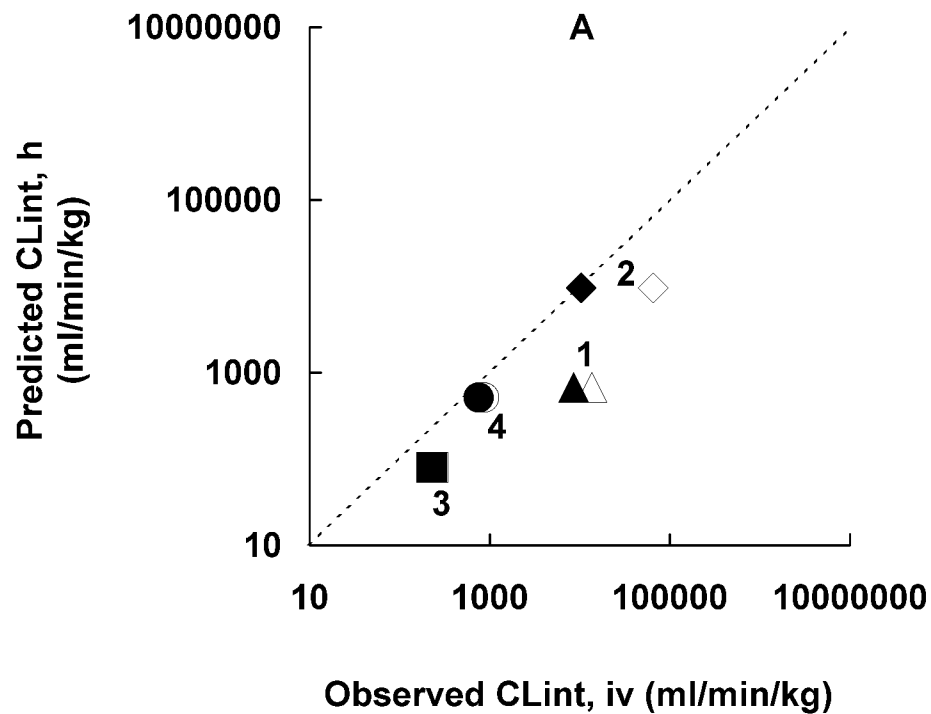
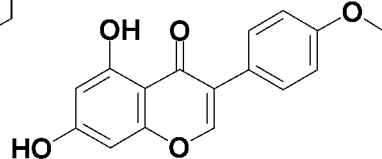


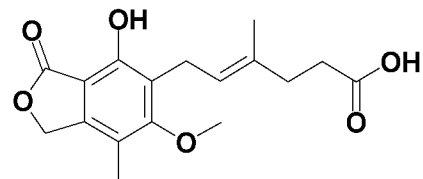
Figure 4



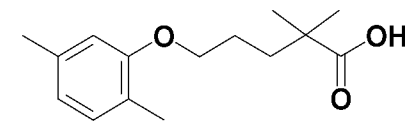
1. Raloxifene



2. Biochanin A



3. Mycophenolic acid



4. Gemfibrozil

Downloaded from dnd.aspejournals.org at ASPET Journals on April 18, 2024

Figure 5

